

Nanometre resolution stepping pattern and structure of acto-myosin-5a at high ATP reveals new mechanism for processive translocation

Yasuharu Takagi¹, Adam Fineberg², Kavitha Thirumurugan³, Neil Billington¹, Joanna Andrecka², Gavin Young², Daniel Cole², James R. Sellers¹, Peter J. Knight³, Philipp Kukura²

Affiliations: ¹Laboratory of Molecular Physiology, NHLBI, National Institutes of Health, Bethesda, Maryland 20892-8015, USA, ²Physical and Theoretical Chemistry Laboratory, Department of Chemistry, University of Oxford, Oxford, OX1 3QZ, UK, ³Astbury Centre for Structural Molecular Biology, and Institute of Molecular and Cellular Biology, University of Leeds, Leeds, LS2 9JT, UK

Abstract

Myosin-5a is a molecular motor that transports cargoes and steps in a symmetric hand-over-hand mechanism along actin, with both heads attached most of the time. By tracking 20 nm gold nanoparticles attached to a single head of the myosin-5a heavy meromyosin-like construct, with sub-nanometer precision via interferometric scattering (iSCAT) microscopy, analysis of stride-sizes showed peaks corresponding to 22, 24, 26, 28, 30, 32 and 34 actin subunits. Kinetic analysis of dwell times determined for different stride sizes at limiting [ATP] showed changes in the ADP release rate for azimuthally strained myosin-5a.

Furthermore, inter-domain coupling of myosin-5a was observed, whereby at the beginning of each stride, the tip of the tail is briefly localized ~32 nm ahead of the next dwell position, as if “leaning forward” along the longitudinal axis of the actin filament. Correlative iSCAT/fluorescence imaging showed this forward leaning transient of the tail domain occurred synchronously with the transient detached state observed for the detached labelled motor domain.

Additionally, we examined full-length myosin-5a by cryo-electron microscopy (EM) in mixtures with actin filaments, flash frozen at saturating [ATP], and observed a population of molecules, usually attached to actin via both heads. Trailing heads, which unlike in earlier studies contain ADP, exhibited a post-powerstroke conformation and straight levers. Leading head levers emerged from the motor domain at a pre-powerstroke position and were gently curved. Supporting the earlier negative stain EM studies of myosin-5a and the iSCAT data, cryo-EM images showed molecules mostly span 13 actin subunits but some span 11 or 15.

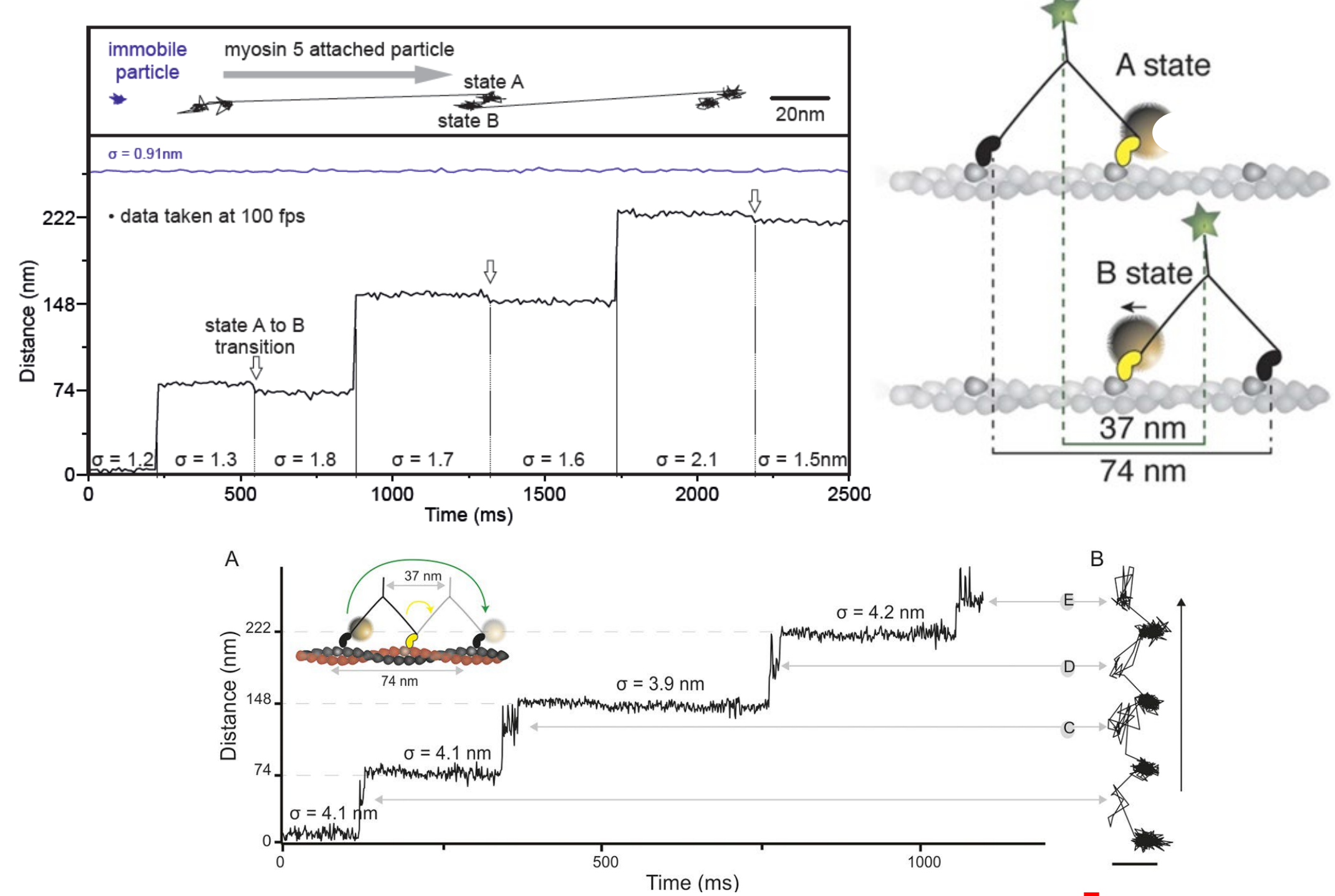
These results suggest a new translocation mechanism of myosin-5a attributable to both the intrinsic structural flexibility of the molecule, as well as the intramolecular gating of load dependent ADP release.

Introduction and motivation of our work

Myosin-5a (M5a) is an unconventional myosin associated with cargo transport. M5a takes ~36 nm steps along actin filaments, matching the 13 actin subunit helical repeat.

We have previously shown using interferometric scattering microscopy (iSCAT) that a M5a with a 20 nm gold particle bound to the motor domain of just one of the two heads, using 5 nm bins for a histogram, shows a single peak ~72 nm, representing the M5a stride, similar to results reported using other dynamic biophysical methods. In addition, we have shown that two states of the bound head exists, from the observation of a backward movement of the gold particle. This motion displays that the labeled motor in the A-state is the leading motor, and in the B-state the labeled motor is the trailing motor when the unlabeled head passes the labeled motor. Furthermore, monitoring the motion of the unbound head precisely revealed a transient state with a center of mass just over half-way between the two binding sites and offset by 40 nm perpendicular to the actin filament. These observations would not have been achieved without the unique and high spatiotemporal precision of iSCAT.

The displacement time series show two states (A and B):



Diagrams from: Andrecka et al, *eLife*, (2015)

Negative stain EM studies have shown that in addition to this 13 subunit separation, that M5a can take 11 and 15 subunit steps. Dynamic biophysical techniques to characterize the step length distribution for a mobile M5a have only exhibited a broad distribution of steps centered around 13 actin subunits (~36 nm). Shorter or longer steps as seen in the negative stain EM studies have not been resolved due to the lack of spatiotemporal resolution.

To address this inconsistency, we revisited the experiments tracking the 20 nm gold particle bound to a single head of the M5a at 10 μ M ATP to take advantage of the unique spatiotemporal precision of iSCAT. Additionally, to complement the iSCAT measurements, we performed cryo-EM at saturating [ATP]. Cryo-EM avoids some of the possible artifacts that exist when using negative stain EM, such as artefacts due to sample support.

Cryo-EM M5a step size distribution show variable step lengths

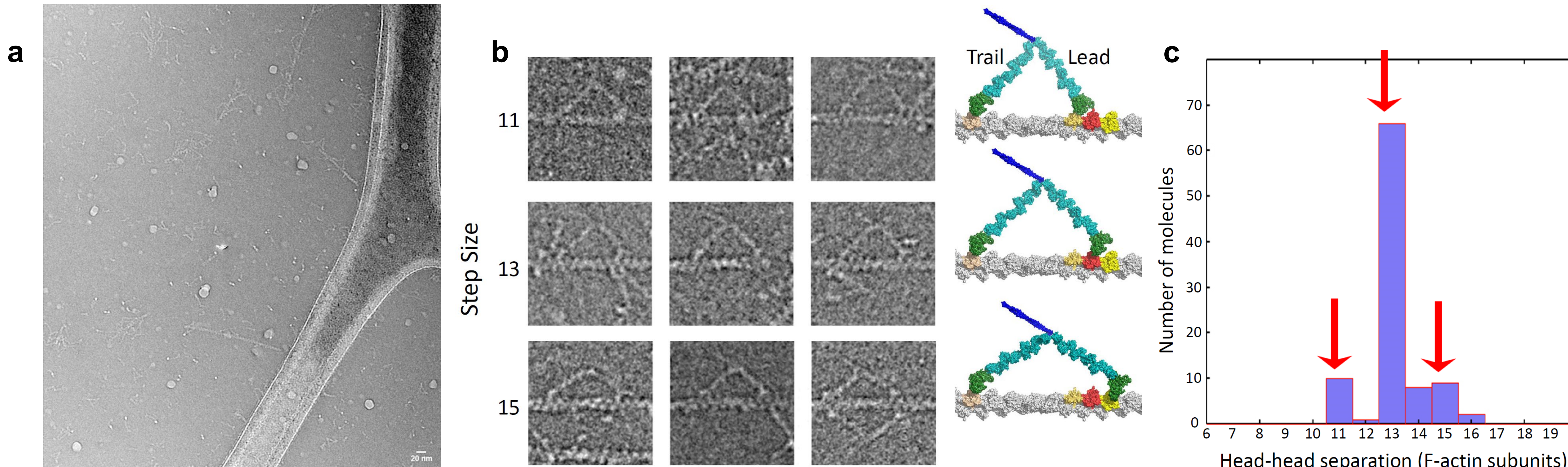


Fig. a: Field of M5a (full length) and F-actin in 0.2 mM ATP. M5a bound by both heads to F-actin can be seen along with compact molecules and extended, detached molecules.

Fig. b: raw images with steps measured at 11, 13 and 15 actin subunits (left), with atomic models of M5a with the same step lengths (right). All molecules are moving to the right. In the model the 11th, 13th and 15th subunits from the trail head are pink, red and yellow respectively

Fig. c: Histogram of measured separation between motor domains. Similarly to negative stain EM, cryo-EM acto-M5a head-head separation shows peaks at 11, 13 and 15 actin subunits.

iSCAT – M5a stride tracking via gold labeling on one head show variability in stride size

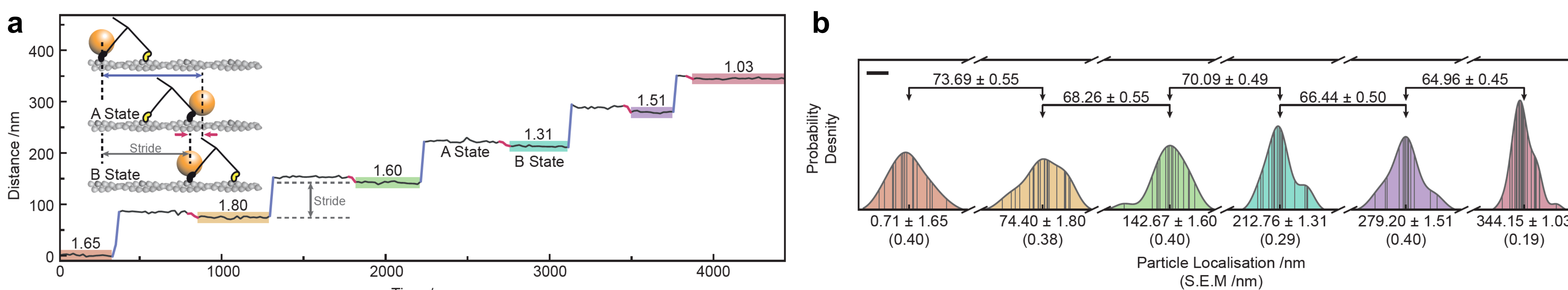


Fig. a: Distance vs. time trace of a gold labeled M5a motor domain highlighting labeled strides (blue) and AB transitions (red). Localization precisions defined as the standard deviation of stationary states marked above each B state. Inset: Schematic of two consecutive myosin strides, highlighting labelled stride and AB transition.

Fig. b: Distributions of localizations highlighted in a with gray vertical lines at each localization. Distances between the means demonstrate high precision of stride size measurements. (Error on particle localizations: standard deviation, error on stride sizes: root sum square of standard error on means; Scale bar: 2 nm).

M5a iSCAT stride distribution show multimodal peaks

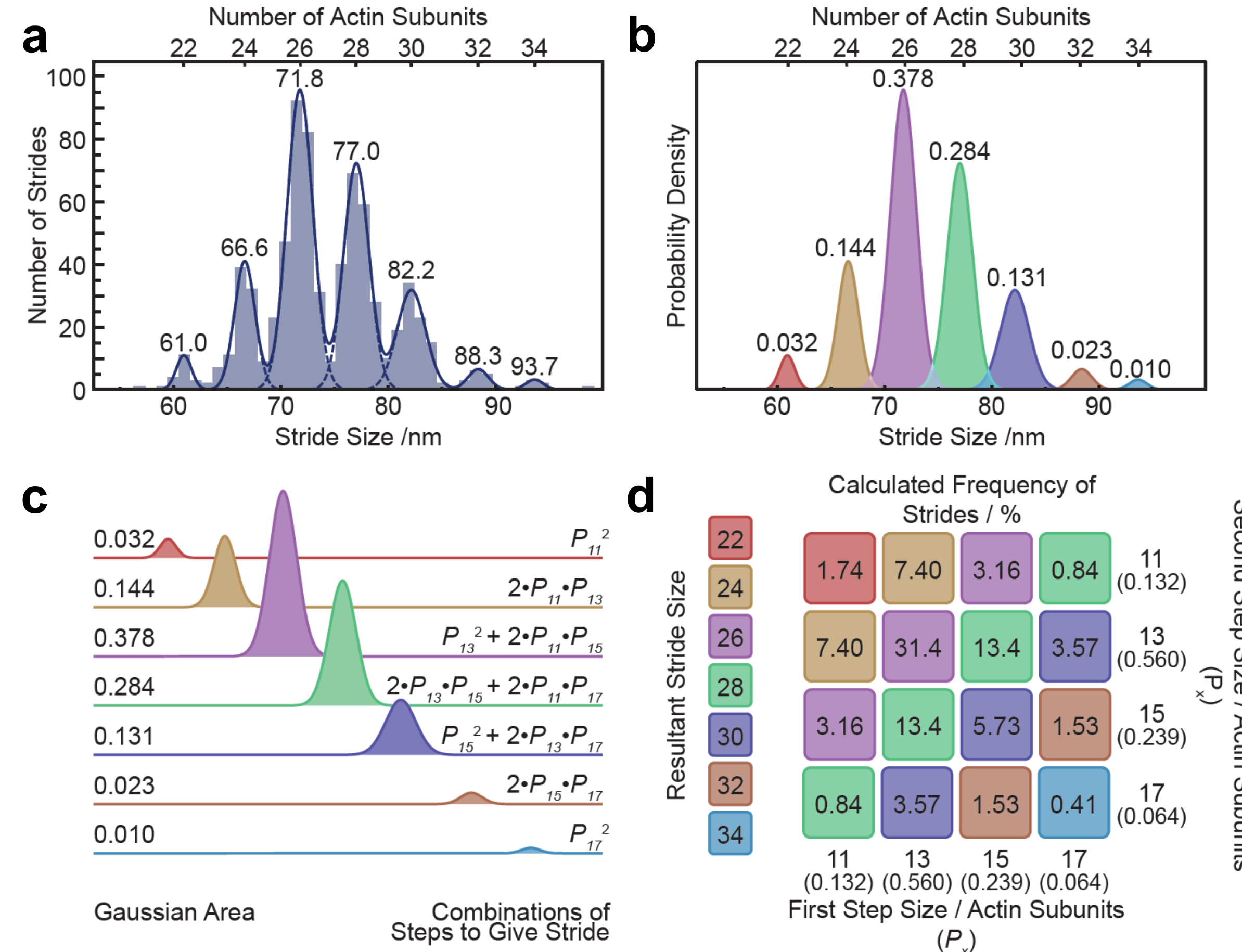


Fig. a: Histogram of M5a strides (N = 96 molecules; 725 strides). A fit of a sum of 7 Gaussians, each with the same fixed width, is shown (solid blue lines), as well as individual Gaussians (dashed blue lines). Mean stride size of each Gaussian (in nm) are labelled above fits, and calculated number of actin subunits traversed marked.

Fig. b: Individual Gaussian fits for each stride size, areas of Gaussians are labelled above the fits.

Fig. c: A schematic illustrating the set of equations used to calculate the probability of a given step size (P_x , $x = 11, 13, 15, 17$) from the areas of the Gaussian fits.

Fig. d: Multiplication grid using the calculated probabilities of each step size (P_x) to determine the frequency of a stride resulting from a given combination of step sizes

M5a iSCAT dwell time distribution show strain dependence

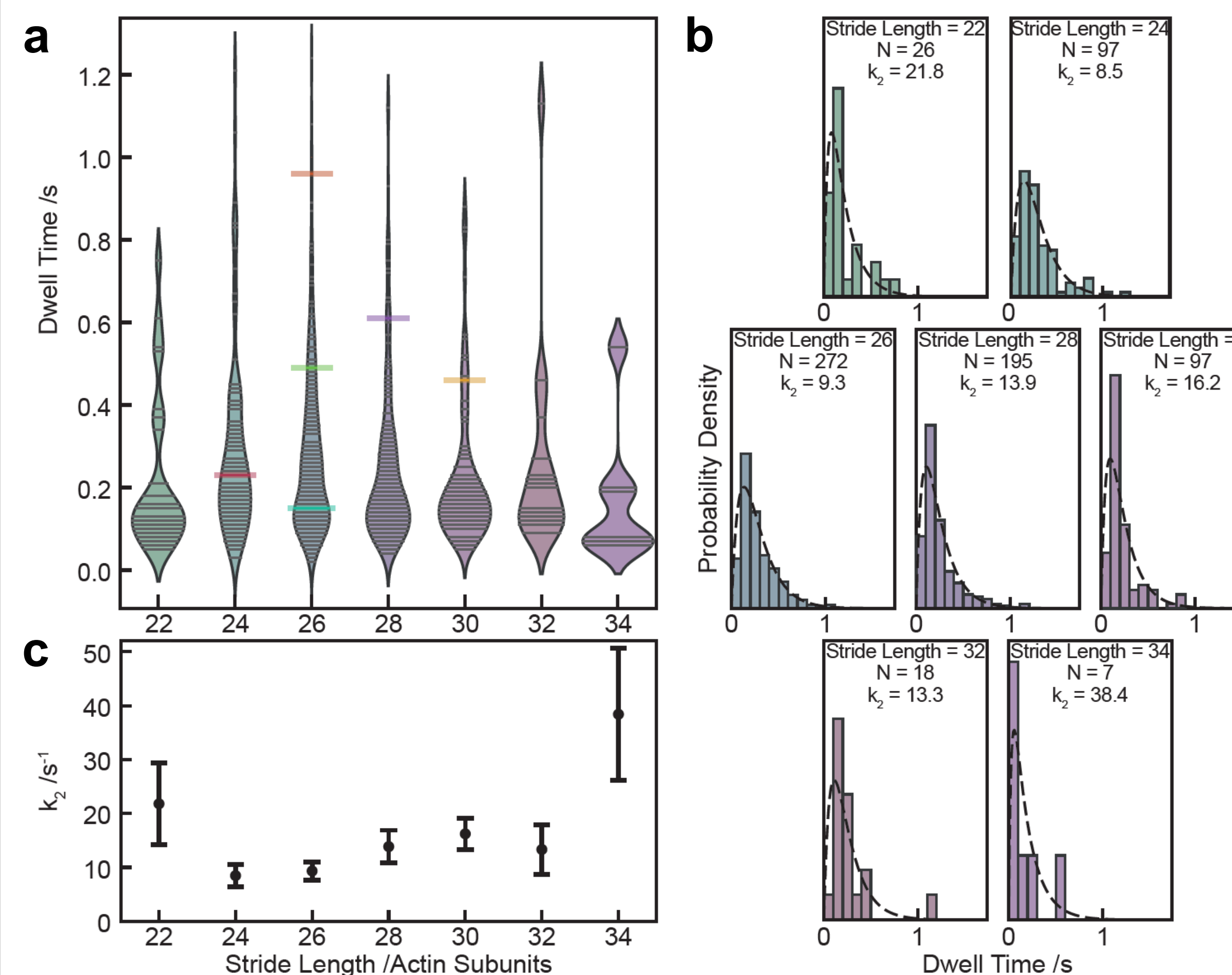


Fig. a: Measured dwell time of A state after stride as a function of stride length. Every data point is shown as a horizontal line. Violin plot envelopes are kernel density estimates of the distributions with bandwidth of 0.15 s.

Fig. b: Dwell time distributions (bars) and results of a global fit (dashed lines) to a double exponential model. k_2 for each stride length is given in the figure. The (shared) k_1 was 5.9 s⁻¹.

Fig. c: Variable rate constant, k_2 , as a function of stride length. Error bars denote the standard error on the mean as determined through 200 bootstrapping iterations.

C-terminus of M5a overshoots by ~34 nm - “Tail flick”

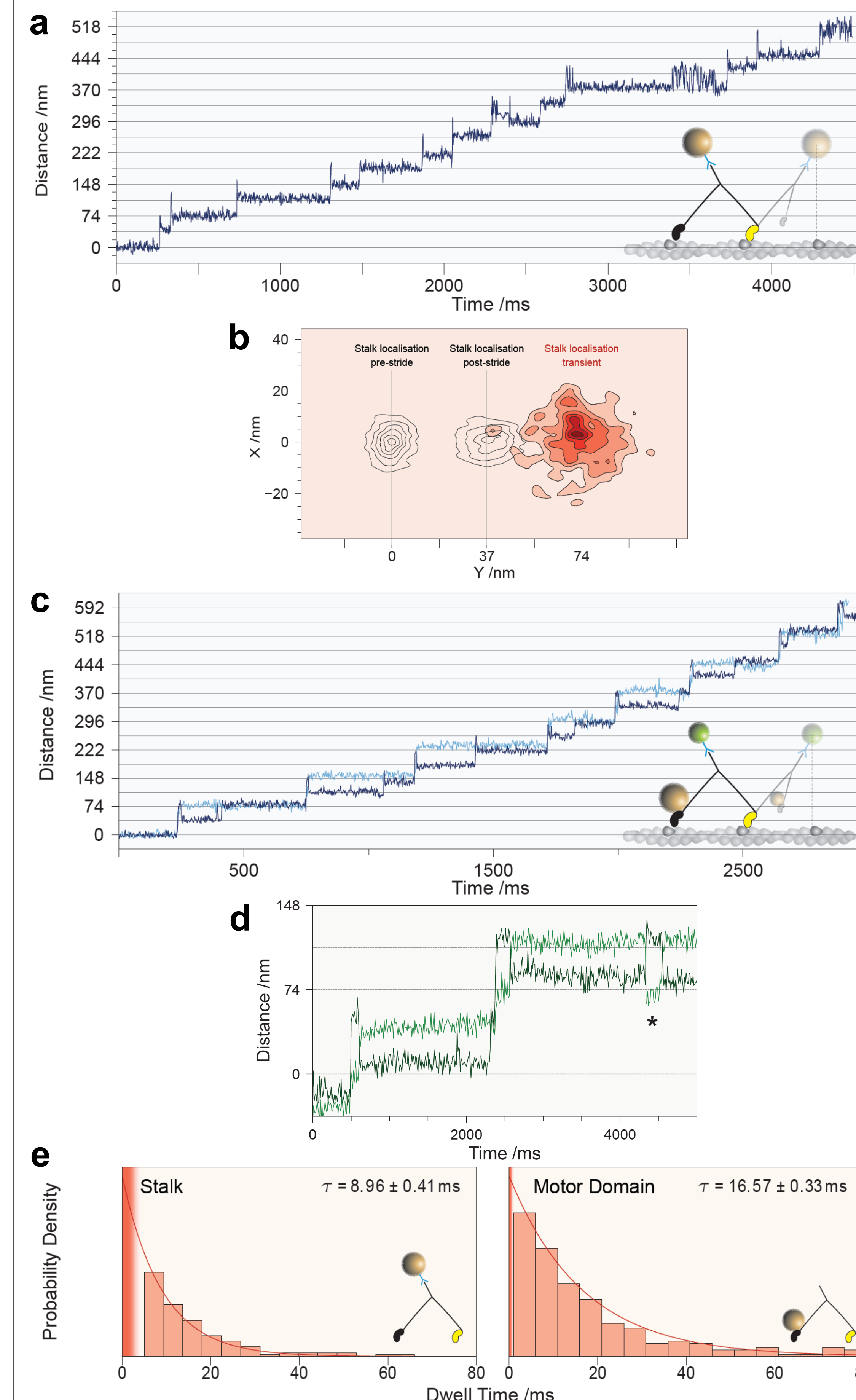


Fig. a: During each step, the stalk leans forward along the longitudinal axis of the actin. The transient state localizes at a position ~34 nm ahead of the post-power stroke dwell position. During a processive run, the stalk can be seen to move back-and-forth between this position and the post-power stroke position.

Fig. b: 2D density estimate of stalk label localizations. The non-shaded densities represents the localizations before (left) and after (right) the step is taken. The shaded density is the localizations of the label whilst in the transient “overshoot” state.

Fig. c: Using simultaneous iSCAT and fluorescence imaging, both the motor domain (dark blue trace) and the stalk (light blue trace) were visualized. The transient state of the stalk occurs synchronously with the transient side state of the motor domain.

Fig. d: During the brief period in which the labelled motor domain (light green trace) returns to the transient side state (*), the stalk (dark green trace) also returns to its transient forward position, suggesting coupling of the two domains through the protein’s structure.

Fig. e: Dwell time analysis of the stalk (left) and the motor (right) domains’ transient states. The lifetime of the stalk is shorter than that for the motor, suggesting the stalk relaxes prior to the motor domain re-binding to the actin. The shaded dark red regions are the length of instrument dead time accounted for in the fit to reduce the effects of under-sampling of short dwell times.

Conclusions

- Both M5a step length and stride are variable.
- iSCAT allows precise determination of stride lengths, within each trajectory.
- M5a is an “imprecise” stepper.
- Dwell times for short (22 subunit) and long (34 subunit) strides are shorter than for others suggesting that azimuthal strain has an effect.
- M5a stalk is rigidly coupled to the motor domain and lever arm allowing strain to transfer through the entire structure.